JEM Journal of Experimental Medicine

ARTICLE

Metabolically activated adipose tissue macrophages link obesity to triple-negative breast cancer

Payal Tiwari[1,2], Ariane Blank[1,2], Chang Cui[1,2], Kelly Q. Schoenfelt[2], Guolin Zhou[2], Yanfei Xu[3], Galina Khramtsova[4], Funmi Olopade[4], Ajay M. Shah[6], Seema A. Khan[3], Marsha Rich Rosner[1,2], and Lev Becker[1,2,5]

Obesity is associated with increased incidence and severity of triple-negative breast cancer (TNBC); however, mechanisms underlying this relationship are incompletely understood. Here, we show that obesity reprograms mammary adipose tissue macrophages to a pro-inflammatory metabolically activated phenotype (MMe) that alters the niche to support tumor formation. Unlike pro-inflammatory M1 macrophages that antagonize tumorigenesis, MMe macrophages are pro-tumorigenic and represent the dominant macrophage phenotype in mammary adipose tissue of obese humans and mice. MMe macrophages release IL-6 in an NADPH oxidase 2 (NOX2)–dependent manner, which signals through glycoprotein 130 (GP130) on TNBC cells to promote stem-like properties including tumor formation. Deleting *Nox2* in myeloid cells or depleting GP130 in TNBC cells attenuates obesity-augmented TNBC stemness. Moreover, weight loss reverses the effects of obesity on MMe macrophage inflammation and TNBC tumor formation. Our studies implicate MMe macrophage accumulation in mammary adipose tissue as a mechanism for promoting TNBC stemness and tumorigenesis during obesity.

Introduction

Obesity is a major modifiable risk factor for breast cancer and is responsible for ∼20% of cancer deaths (Calle et al., 2003). In addition to its role in breast cancer pathogenesis, obesity is recognized as a marker of poor prognosis in pre- and postmenopausal women (Chan and Norat, 2015). Epidemiological studies have linked obesity with increased risk of developing different subtypes of breast cancer, including triple-negative breast cancer (TNBC; Vona-Davis et al., 2008; Trivers et al., 2009; Pierobon and Frankenfeld, 2013), a particularly aggressive form of breast cancer with poor outcome and few therapeutic options. Among TNBC patients, progression- and disease-free survival are strongly correlated with obesity (Choi et al., 2016). However, mechanisms by which obesity leads to worsened TNBC prognosis are incompletely understood.

One clue to its action is that obesity causes chronic inflammation. Recent studies showed that obesity-induced neutrophil accumulation in the lung promotes breast cancer metastasis (Quail et al., 2017). In addition to inflammation at metastatic sites, obesity also promotes local inflammation in adipose tissue that is mediated by macrophage infiltration and activation (Xu et al., 2003; Lumeng and Saltiel, 2011). Obesity-induced inflammation in mammary adipose tissue (Howe et al., 2013; Vaysse et al., 2017) may be of particular significance because breast cancers form in this niche, and inflammation promotes stem-like properties in cancer cells and an increased propensity to form tumors (Grivennikov et al., 2010). Thus, pro-inflammatory macrophage accumulation in mammary fat may augment TNBC tumor formation during obesity.

Pro-inflammatory macrophages have often been associated with a classically activated (M1) phenotype, which activates the immune response and opposes tumorigenesis (Pyonteck et al., 2013). In contrast, anti-inflammatory macrophages are considered to adopt an alternatively activated phenotype that attenuates immunity and promotes tumorigenesis (Noy and Pollard, 2014). Earlier studies showed that obesity promotes an M1-like phenotype in adipose tissue macrophages (ATMs) in visceral fat (Lumeng et al., 2007), which would be expected to oppose tumor formation. However, more recent studies challenged this paradigm (Xu et al., 2013; Kratz et al., 2014).

Studies from our group showed that obesity produces a pro-inflammatory "metabolically activated" (MMe) ATM phenotype that is both mechanistically and functionally distinct from the

[1]Committee on Cancer Biology, The University of Chicago, Chicago, IL; [2]Ben May Department for Cancer Research, The University of Chicago, Chicago, IL; [3]Department of Surgery and Robert H. Lurie Comprehensive Cancer Center, Feinberg School of Medicine of Northwestern University, Northwestern University, Chicago, IL; [4]Center for Clinical Cancer Genetics and Global Health, Department of Medicine, The University of Chicago, Chicago, IL; [5]Committee on Molecular Metabolism and Nutrition, The University of Chicago, Chicago, IL; [6]School of Cardiovascular Medicine and Sciences, King's College, London British Hearth Foundation Centre, London, UK.

Correspondence to Lev Becker: levb@uchicago.edu; Marsha Rich Rosner: mrosner@uchicago.edu.

M1 phenotype (Kratz et al., 2014; Coats et al., 2017). The MMe phenotype is driven by saturated fatty acids (e.g., palmitate) released by insulin-resistant adipocytes during obesity. Although we showed that MMe macrophages accumulate in visceral and subcutaneous adipose tissue of obese humans and mice, their presence in mammary fat and their role in TNBC tumorigenesis have not been explored.

Here, we show that MMe macrophages accumulate in mammary fat of obese mice and humans. We demonstrate that MMe macrophages secrete IL-6 in a nicotinamide adenine dinucleotide phosphate oxidase 2 (NOX2)–dependent manner that signals through glycoprotein 130 (GP130) on murine and human TNBC cells to promote stem-like properties and tumor formation during obesity. These findings reveal an important mechanism by which obesity enhances TNBC tumorigenesis.

Results

Diet-induced obesity (DIO) promotes TNBC stemness and tumor formation

To determine if DIO promotes TNBC tumorigenesis, we first studied genetically engineered C3(1)-TAg mice, which spontaneously develop TNBC-type tumors in multiple mammary glands (Green et al., 2000). Female C3(1)-TAg mice on the FVB/N background were fed a low-fat diet (LFD) or high-fat diet (HFD) for 12 wk. Although FVB/N mice are somewhat protected from DIO (Montgomery et al., 2013), HFD-fed mice had increased body weight, fasting glucose, and mammary/visceral fat pad weight compared with LFD-fed mice (Fig. 1, A–C).

As previously reported (Mustafi et al., 2017), DIO increased the total tumor burden in C3(1)-TAg mice (Fig. 1 D), and this increased burden was due, in part, to the presence of more tumors in obese mice (Fig. 1 E), suggesting that DIO may promote tumor initiation in a genetically engineered mouse model of TNBC.

The tumor-initiating capacity of cancer cells has been linked to their stem-like properties (Nguyen et al., 2012). We therefore quantified the expression of stem-associated markers in cancer cells isolated from lean and obese C3(1)-TAg mice. We found that DIO increased the expression of *Sox2*, *Oct4*, and *Nanog* (Klonisch et al., 2008) and cell surface CD90 levels (Lu et al., 2014) in cancer cells (Fig. 1, F and G; and Fig. S1), suggesting that obesity may create an environment that enhances stemness in TNBC cells.

To test this possibility, we switched to a syngeneic orthotopic transplant model in obesity-prone C57BL/6 mice. This model allowed us to establish an obese environment, and then determine whether this preexisting environment is more capable of supporting the tumor-initiating potential of TNBC cells, a key function ascribed to cancer stem cells.

We fed female C57BL/6 mice an LFD or HFD for 12 wk to induce obesity, hyperglycemia, and mammary and visceral fat expansion (Fig. 1, H–K). At this time, murine E0771 or Py8119 TNBC cells were injected at limiting dilutions into mammary fat pads of lean or obese mice, diets were continued, and their tumor-initiating potential was assessed using a limiting dilution assay. We found that DIO decreased the number of E0771 or Py8119 cells required to form tumors (Fig. 1 L) as well as tumor latency (Fig. S2), reinforcing the notion that obesity promotes TNBC tumor formation.

The ability of DIO to promote the tumor-initiating potential of TNBC cells could be due to high nutrient levels that support tumor growth, or due to some other change induced by chronic high-fat feeding. To differentiate between these possibilities, we fed female C57BL/6 mice an LFD or HFD for 4 d to create conditions of nutrient excess without changes in body weight, fasting glucose, or mammary/visceral adipose tissue mass (Fig. 1, H and M–O). At this time, we injected E0771 or Py8119 cells into mammary fat, continued diet feeding, and quantified tumor incidence over a 7-wk period.

Short-term preexposure to HFD did not support increased E0771 or Py8119 tumor formation (Fig. 1 L), even though mice were maintained on the HFD for 7 wk following tumor cell injection. These data suggest that the induction of TNBC tumor-initiating potential requires a state of preexisting obesity and is not simply reliant on nutrient excess.

Obese mammary ATMs (mATMs) induce stem-like properties in TNBC cells

Obesity has been characterized as a chronic inflammatory state (Lumeng and Saltiel, 2011), and pro-inflammatory cytokines have been shown to enhance the tumor-initiating potential of many types of cancer cells (Nguyen et al., 2012). ATMs are an important source of cytokines during obesity, and they are in close proximity to early ductal carcinoma in situ (DCIS) in obese C3(1)-TAg mice (Fig. 1 P). Moreover, resident ATMs in mammary fat have been implicated in supporting the development of stem cells and cancer stem cells (Gyorki et al., 2009; Chakrabarti et al., 2018). We therefore hypothesized that an increase in pro-inflammatory ATMs in mammary fat might help to explain how DIO promotes TNBC tumor formation.

To begin to test this hypothesis, we determined whether DIO could increase the number of mammary fat ATMs and/or their pro-inflammatory cytokine expression in female C57BL/6 mice fed the HFD for 12 wk. Although DIO substantially increased mammary adipose tissue mass, the percentage of $CD45^+$ immune cells, ATMs (defined as $CD11b^+F4/80^+$), and $CD4^+$ and $CD8^+$ T cells in the stromal vascular cells (SVCs) were not increased (Fig. 2 A and Fig. S1).

To examine the inflammatory status of mATMs, we purified them from lean and obese mice (Fig. 2 B) and measured the expression of *Tnfa*, *Il1b*, and *Il6*, inflammatory cytokines commonly found to be elevated in ATMs during obesity (Xu et al., 2003; Lumeng et al., 2007; Kratz et al., 2014). We found that mATMs from obese mice had elevated pro-inflammatory cytokine expression in comparison to those from lean mice (Fig. 2 C). Thus, although DIO did not induce mATM accumulation in mice, it did increase ATM inflammation in mammary fat; the latter observation is similar to what has been widely reported in visceral fat depots (Xu et al., 2003; Lumeng et al., 2007; Kratz et al., 2014).

Next, we determined whether obese mATMs support stem-like properties in TNBC cells. To explore this, we collected conditioned media from an equal number of mATMs from lean

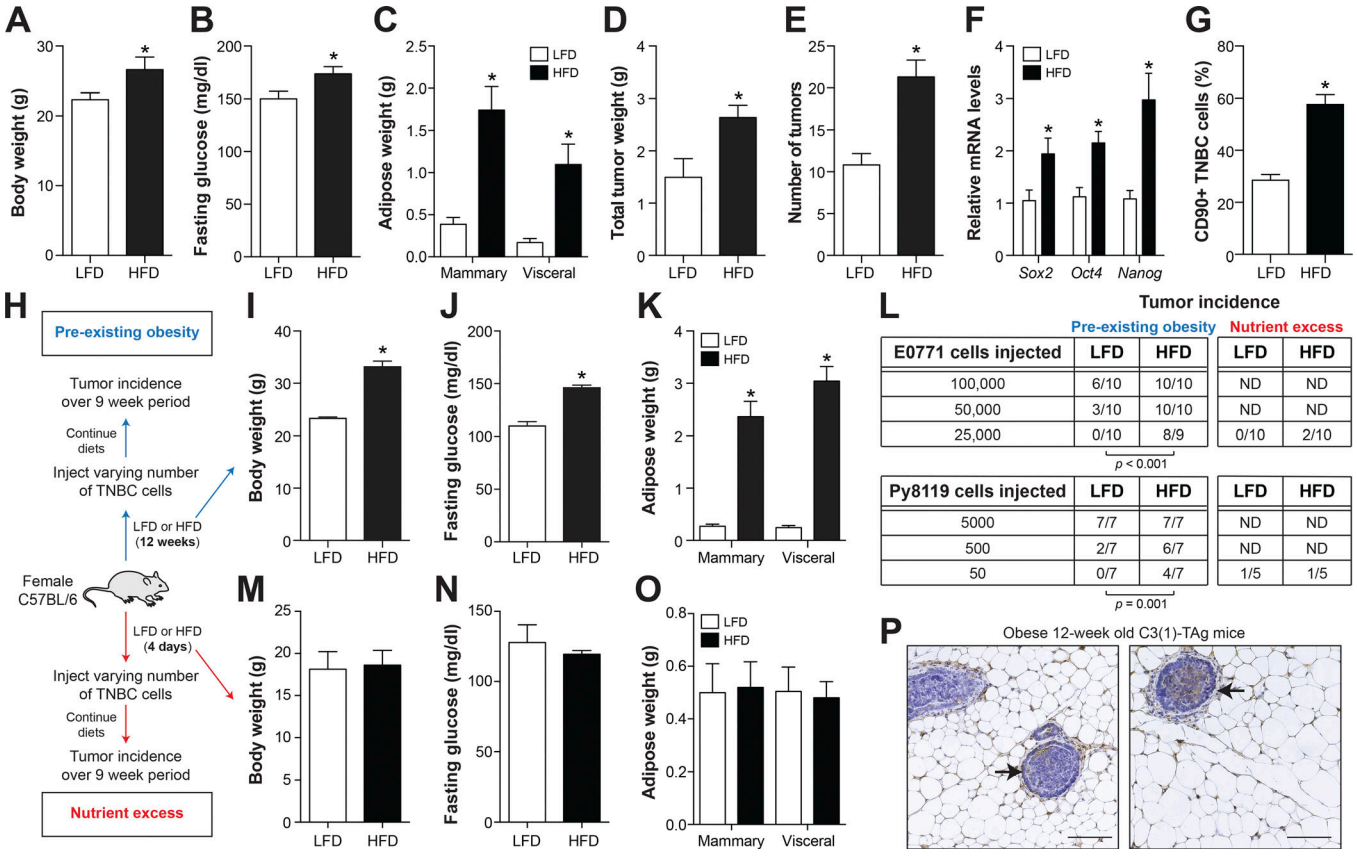

Figure 1. **DIO promotes TNBC cell tumor formation. (A–G)** Female C3(1)-TAg mice were fed a LFD or HFD for 12 wk. **(A)** Body weight, *n* = 10/group. **(B)** Fasting glucose levels, *n* = 10/group. **(C)** Mammary and visceral adipose tissue weight, *n* = 10/group. **(D)** Total tumor weight in all mammary tumors, *n* = 10/group. **(E)** Number of mammary tumors/mouse, *n* = 10/group. **(F and G)** Cancer cells were isolated from tumors and assessed for stem cell marker gene expression by qRT-PCR (F) and CD90 levels by flow cytometry, *n* = 5/group (G). **(H)** Female C57BL/6 mice were fed a LFD or HFD for 12 wk to create preexisting obesity or 4 d to create nutrient excess. Mice were injected with varying TNBC cells into the no. 4 mammary fat pad, diets were continued for 9 wk, and tumor incidence was recorded. **(I–K and M–O)** Body weights, *n* = 15/group (I and M), fasting glucose levels, *n* = 8/group (J and N), and mammary/visceral adipose tissue mass, *n* = 8/group (K and O), were all measured before TNBC cell injection. **(L)** Limiting dilution assay of E0771 or Py8199 cells injected into the no. 4 mammary fat pad of mice, *n* = 5–10/group. Statistical significance for tumor initiation was assessed by ELDA software. **(P)** 6-wk-old C3(1)-TAg mice were fed a HFD for 6 wk. Mammary fat was stained with anti-F4/80 (macrophage marker, brown) and counterstained with hematoxylin (blue) to visualize DCIS (arrow). Bar, 100 µm. Results are mean ± SEM. *, P < 0.05; Student's *t* test.

and obese mice and determined whether this media could (1) induce the expression of stem cell-associated markers in TNBC cells and (2) promote TNBC cell tumorsphere formation, a functional assay associated with cancer stem cells (Lee et al., 2016).

Whereas treatment with conditioned media from lean mATMs had no effect on stem cell marker expression in E0771 cells, conditioned media from obese mATMs increased the percentage of $CD90^+CD24^+$ cells, and the expression of *Sox2*, *Oct4*, and a wide range of stem cell–associated genes including *Nrsf5*, *Sox10*, *Aldh1a1*, *Abcg1*, *Snai1*, *Foxd3*, *Aldh2*, *Lin28*, *Thy1*, and *Sem6a* (Celià-Terrassa et al., 2017; Fig. 2, D and E; and Fig. S1). Obese mATM media also induced tumorsphere formation of E0771 and M6C cells (derived from C3(1)-TAg mice), and this effect was maintained in serially passaged tumorspheres in the absence of continued exposure to ATM media (Fig. 2, F and G; and Fig. S3). In contrast, lean mATM media could not induce tumorsphere formation (Fig. 2 F). Moreover, pretreating E0771 cells with obese mATM media increased their tumor-initiating potential in vivo (Fig. 2 H). Together, these findings suggest that obesity reprograms mATMs to promote stem-like properties in TNBC cells, consistent with a pro-tumorigenic phenotype.

Obese mATMs adopt an MMe phenotype

Next, we explored the nature of the pro-inflammatory mATM phenotype in obese mice. Although we previously showed that MMe macrophages are present in visceral and subcutaneous adipose tissue depots in obese humans and mice (Kratz et al., 2014), their presence in mammary adipose tissue has not been investigated. This is important because obesity can elicit substantially diverse effects on different adipose tissue depots (Wang et al., 2013).

We used two approaches to determine whether obesity induced an MMe-like phenotype in mATMs. First, we compared mATMs from lean and obese female C57BL/6 mice for the expression of markers diagnostic of the M1 (*Cd40*, *Cd38*) and MMe (*Cd36*, *Plin2*) phenotypes (Kratz et al., 2014). We

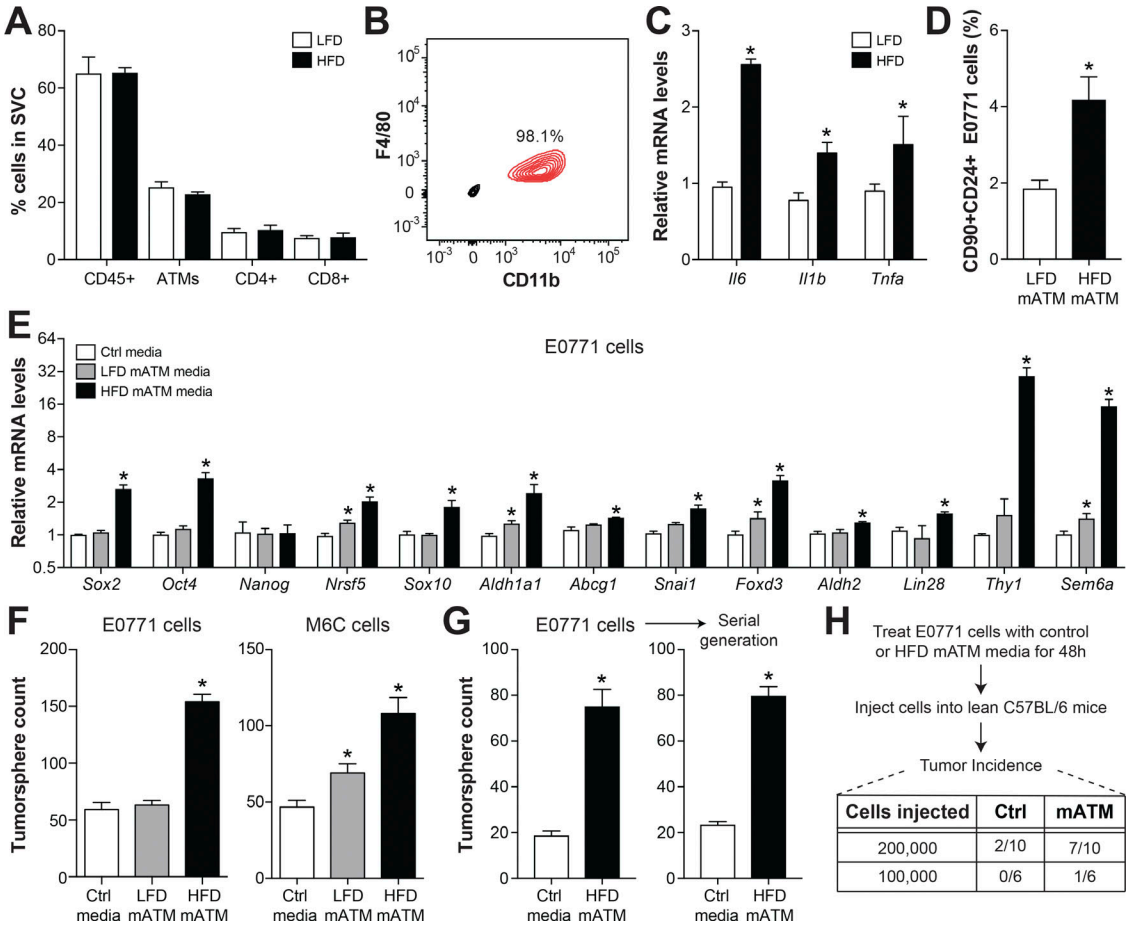

Figure 2. **Obese mATMs promote stem-like properties in TNBC cells.** Female C57BL/6 mice were fed a LFD or HFD for 12 wk. **(A)** Immune cell composition in the SVCs from mammary adipose tissue was assessed by flow cytometry: ATMs (F4/80$^+$CD11b$^+$), T cells (CD3$^+$CD4$^+$ or CD3$^+$CD8$^+$), *n* = 4/group. **(B)** Purity of mATMs isolated from mice. **(C)** Pro-inflammatory cytokine expression in mATMs, *n* = 4/group. **(D–H)** TNBC cells were treated with control media (Ctrl) or media conditioned by mATMs from lean (LFD mATM) or obese (HFD mATM) mice, *n* = 3/group. **(D)** CD90/CD24 levels in E0771 cells, *n* = 3/group. **(E)** Stem cell marker expression in E0771 cells, *n* = 3/group. **(F)** Tumorsphere formation in E0771 and M6C cells, *n* = 4/group. **(G)** Left: Tumorsphere formation in E0771 cells treated with HFD mATM media. Right: E0771 cells were isolated and assessed for serially generated tumorsphere formation in the absence of HFD mATM media, *n* = 3/group. **(H)** Tumor incidence following injection of E0771 cells into the no. 4 mammary fat pad of lean C57BL/6 mice, *n* = 6–10/group. Ctrl, control. Results are mean ± SEM. *, P < 0.05; Student's *t* test.

found that obesity induced the expression of MMe markers, but not M1 markers, in mATMs (Fig. 3 A). These findings suggest that the milder DIO that develops in female mice (Dorfman et al., 2017) is sufficient to support an MMe phenotype in ATMs, and that MMe, rather than M1, is the dominant pro-inflammatory macrophage phenotype in mammary adipose tissue of obese mice.

Second, we determined whether in vitro–derived, palmitate-treated MMe macrophages could mimic the stem cell–promoting properties of obese mATMs. Conditioned media from MMe macrophages induced the expression of *Oct4* and *Nanog* and the percent CD90$^+$CD24$^+$ E0771 cells (Figs. S1 and S4). MMe media also promoted tumorsphere formation in E0771 and M6C cells (Fig. 3 C and Fig. S3) and tumor-initiating potential of E0771 cells in vivo (Fig. 3 D).

Together, these findings show that obese mATMs express markers of MMe rather than M1 macrophages, and that in vitro–derived MMe macrophages mimic their effects on TNBC stem-like properties.

MMe mATMs contribute to the enhanced TNBC tumor formation in obese mice

To determine whether MMe ATMs contribute to TNBC tumorigenesis during obesity, we took advantage of our previous work, which showed that NOX2 is required for the induction of pro-inflammatory cytokines in MMe macrophages, but not M1 macrophages (Coats et al., 2017).

We first determined whether deleting NOX2 (*Cybb*$^{-/-}$) in in vitro–derived MMe macrophages could diminish their ability to promote TNBC stem-like properties. As previously described, deleting *Nox2* lowered inflammatory cytokine expression in MMe macrophages (Fig. 3 E). Moreover, deleting *Nox2* in MMe macrophages attenuated their ability to induce stem cell–associated marker expression and tumorsphere formation in E0771 cells in vitro (Figs. 3, F and G; and Fig. S3). Thus, the pro-inflammatory and stem cell–promoting properties of in vitro–derived MMe macrophages are dependent on *Nox2*.

Next, we determined whether *Nox2* is required in vivo. We fed myeloid cell–specific *Nox2*-deficient mice (m*Nox2*$^{-/-}$) and

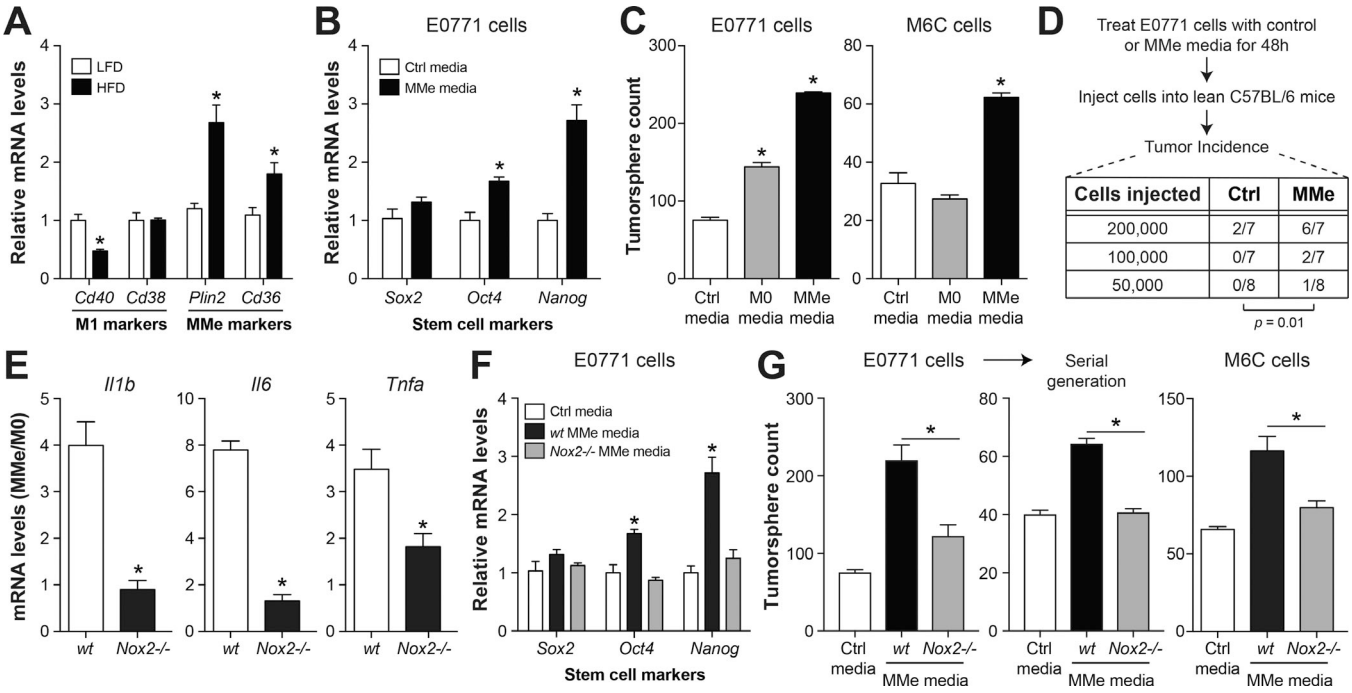

Figure 3. **Obese mATMs adopt a MMe phenotype. (A)** M1 and MMe marker expression in mATMs from lean and obese C57BL/6 mice, *n* = 4/group. **(B–D)** BMDMs (M0) were MMe in vitro. Effect of MMe macrophage media on E0771 stem cell marker expression, *n* = 3/group (B), E0771 and M6C cell tumorsphere formation, *n* = 3/group (C), and tumor incidence following injection of E0771 cells into the no. 4 mammary fat pad, *n* = 7–8/group (D). Ctrl, control. **(E–G)** WT and Nox2$^{-/-}$ BMDMs were MMe in vitro. **(E)** Cytokine expression in MMe macrophages, *n* = 3/group. **(F and G)** Effect of MMe macrophage media on E0771 stem cell marker expression, *n* = 3/group (F), E0771 and M6C cell primary tumorsphere formation, and serially generated E0771 cell tumorsphere formation, *n* = 3/group (G). Results are mean ± SEM. *, P < 0.05; Student's *t* test. Statistical significance for tumor initiation was assessed by ELDA software.

littermate controls (WT) a HFD for 12 wk. As previously described in male m*Nox2*$^{-/-}$ mice (Coats et al., 2017), female m*Nox2*$^{-/-}$ mice fed a HFD gained more body weight and adipose tissue mass than WT mice (Fig. 4, A and B). However, fasting glucose and insulin levels were unaffected (Fig. 4, C and D). Mammary and visceral adipose tissue health and liver fat accumulation were also unaffected (Fig. S3), which is important because, in males, m*Nox2*$^{-/-}$ mice develop late-onset visceral lipoatrophy and hepatosteatosis after 16 wk of HFD (Coats et al., 2017).

Although the percentage of mATMs was elevated in m*Nox2*$^{-/-}$ mice (Fig. 4 E), analysis of these ATMs revealed attenuated expression of all MMe markers tested, including *Tnfa*, *Il6*, *Il1b*, *Cd36*, and *Plin2* (Fig. 4 F). Thus, female m*Nox2*$^{-/-}$ mice afford an opportunity to study the role of MMe macrophages in TNBC tumor formation during DIO in the absence of substantive changes to the obesity phenotype.

Two lines of evidence based on deleting *Nox2* in myeloid cells implicated MMe macrophages in promoting TNBC tumor formation. First, deleting *Nox2* from mATMs decreased their ability to promote stem cell marker expression and tumorsphere formation in E0771 cells (Fig. 4, G and H). Second, deleting *Nox2* from myeloid cells decreased tumor incidence in obese mice injected with E0771 or Py8119 cells (Fig. 4 I). This decreased tumor incidence was not absolute, which may be explained by (1) the slight increases in body weight, mammary fat mass, and mATM number in m*Nox2*$^{-/-}$ mice and (2) the inability of *Nox2* deletion to completely block the induction of stem-like properties in TNBC cells.

MMe macrophages secrete IL-6, which promotes TNBC stemness through GP130 signaling

Previous studies showed that pro-inflammatory cytokines bind GP130 to induce STAT3 phosphorylation which, in turn, promotes the stem-like properties of many types of cancer cells (Korkaya et al., 2011). One well-studied GP130 ligand is IL-6, whose expression is elevated in MMe mATMs from obese mice (see Fig. 3 C). Because IL-11, oncostatin M (OSM), leukemia inhibitor factor (LIF), ciliary neurotrophic factor (CNTF), and CTF1 can also signal through GP130 (Silver and Hunter, 2010), we examined their regulation in mATMs, and found that obesity increased their transcript expression (Fig. 5 A). Moreover, treating E0771 or M6C cells with obese mATM-conditioned media induced STAT3 phosphorylation (Fig. 5, B and C), a key effector of GP130 signaling.

To further test this, we isolated mATMs from WT and m*Nox2*$^{-/-}$ mice, a perturbation that attenuates both the MMe phenotype of mATMs and the ability of obesity to promote tumor formation. We found that m*Nox2*$^{-/-}$ mATMs had decreased GP130 ligand expression (Fig. 5 A) and diminished capability to induce STAT3 phosphorylation in E0771 cells (Fig. 5 C). In vitro–derived MMe macrophages similarly up-regulated the expression of all GP130 ligands tested, and their media also induced STAT3 phosphorylation in E0771 and M6C cells in a

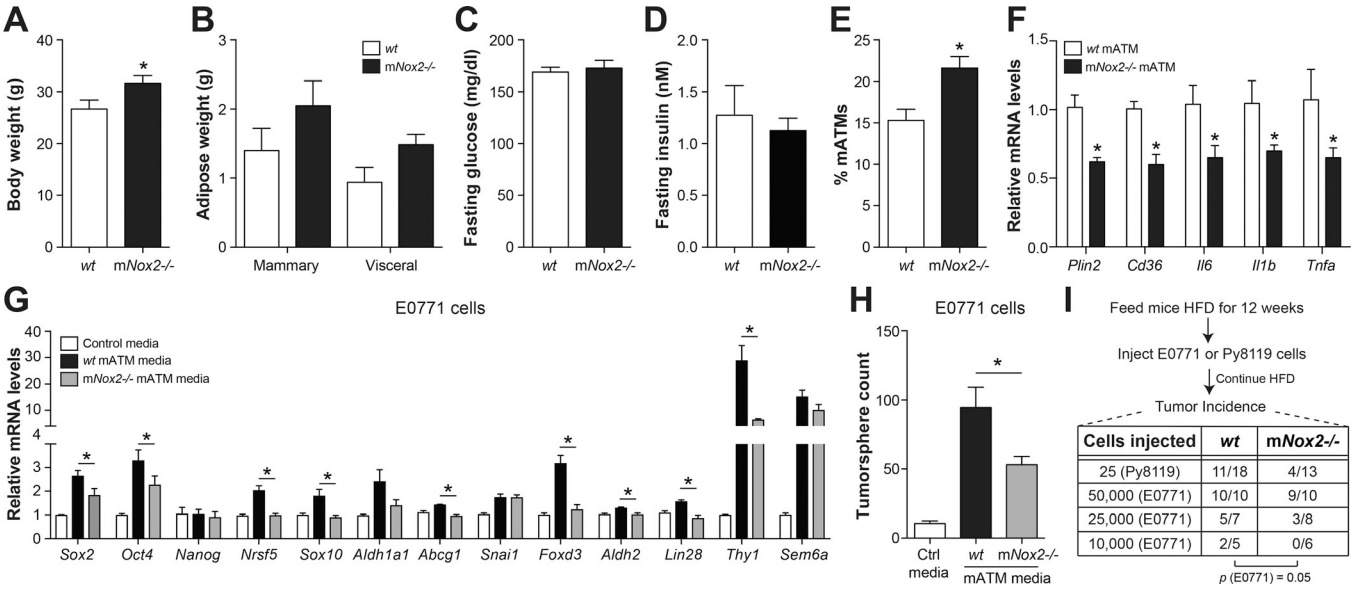

Cells injected	wt	mNox2-/-
25 (Py8119)	11/18	4/13
50,000 (E0771)	10/10	9/10
25,000 (E0771)	5/7	3/8
10,000 (E0771)	2/5	0/6

Figure 4. **MMe ATMs contribute to the enhanced TNBC cell tumor formation during obesity.** Control *Nox2*$^{fl/fl}$ mice (WT) and myeloid cell-specific LysM-cre$^{+/-}$ *Nox2*$^{fl/fl}$ mice (m*Nox2*$^{-/-}$) were fed a HFD for 12 wk. **(A)** Body weight, *n* = 8/group. **(B)** Mammary and visceral adipose tissue weight, *n* = 8/group. **(C and D)** Fasting glucose and insulin levels, *n* = 8/group. **(E)** Percentage of ATMs (CD11b$^+$F4/80$^+$) in mammary adipose tissue, *n* = 3/group. **(F)** MMe marker expression in mATMs, *n* = 3/group. **(G and H)** Effects of mATM media on E0071 stem cell marker expression, *n* = 3/group (G), and tumorsphere formation, *n* = 3/group (H). Ctrl, control. **(I)** Tumor incidence following injection of E0771 or Py8199 cells into the no. 4 mammary fat pad, *n* = 5–18/group. Results are mean ± SEM. *, P < 0.05; Student's *t* test. Statistical significance for tumor initiation was assessed by ELDA software.

GP130-dependent manner (Fig. S4), suggesting that this pathway may be used by MMe macrophages to promote stem-like properties in TNBC cells.

Next, we determined if one of the GP130 ligands was most important for driving TNBC stemness. We treated obese mATM media with inactivating antibodies against IL-6, IL-11, OSM, LIF, or CTF1, alone or in combination, and monitored effects on STAT3 phosphorylation in E0771 cells. Results showed that the IL-6 neutralizing antibody was the only antibody that attenuated STAT3 phosphorylation (Fig. 5 D). Moreover, purified IL-6 was sufficient to induce tumorsphere formation in E0771 cells (Fig. 5 E). Finally, IL-6 protein levels were elevated twofold in obese relative to lean mATM media (Fig. 5 F). These findings suggest that MMe macrophage-derived IL-6 plays a prominent role in driving TNBC cell stemness. However, we cannot rule out a contribution from other factors, since IL-6 neutralization did not completely abrogate the MMe macrophage-induced stem cell phenotype.

We then determined whether GP130 is required for obese mATMs to promote stem-like properties in TNBC cells. To test this, we used shRNA to knock down GP130 levels in E0771 cells, confirmed knockdown using several clones (Fig. 5 G), and studied effects of obese mATMs on TNBC cells. We found that knocking down GP130 attenuated the ability of obese mATM media to induce STAT3 phosphorylation and increase stem cell marker expression in E0771 cells (Fig. 5, H and I).

We further explored whether GP130 signaling was required for DIO to promote the tumor-initiation potential of TNBC cells in vivo by injecting short hairpin (sh)–control or sh-*Gp130* E0771 cells into obese female mice and monitoring tumor incidence. *Gp130* knockdown in E0771 cells attenuated the ability of obesity to promote tumor formation in vivo (Fig. 5 J), and this decrease was comparable to the effect observed in obese m*Nox2*$^{-/-}$ mice (see Fig. 4 I).

Weight loss reduces MMe macrophage inflammation and TNBC tumor formation in mammary fat

Our findings suggest that DIO increases MMe macrophages in mammary fat, which overexpress IL-6 that signals through GP130 to promote TNBC tumor formation. Given the relevance of weight loss as a noninvasive therapeutic strategy for patients, we investigated whether weight loss could reverse this pathway in obese mice. To test this, we fed female C57BL/6 mice the HFD for 3 mo, and then switched them to the LFD for 5 wk to induce weight loss (Fig. 6 A). As a control, we fed mice the LFD for the entire duration. As expected, switching to the LFD reduced body weight to a stable level, normalized fasting glucose, and lowered mammary and visceral fat mass (Fig. 6, A–D).

Analyses of mATMs from the mice showed that weight loss completely reversed their expression of IL-6 as well as other GP130 ligands and inflammatory cytokines (Fig. 6 E). However, *Cd36* and *Plin2* levels remained elevated in mATMs (Fig. 6 E), perhaps due to the excess free fatty acid (FFA) released by adipocytes during weight loss. Indeed, our previous studies showed that excessive FFAs leads to lipid accumulation in MMe macrophages, which attenuates TLR2-dependent inflammatory cytokine expression and induces lipid metabolism genes (e.g., *Cd36* and *Plin2*) through PPARγ and P62 activation (Kratz et al., 2014). Importantly, we found that weight loss eliminated the increased tumor-forming capability of E0771 cells during obesity (Fig. 6 F). Together, these data suggest that weight loss can reverse MMe macrophage inflammation and TNBC tumor formation in

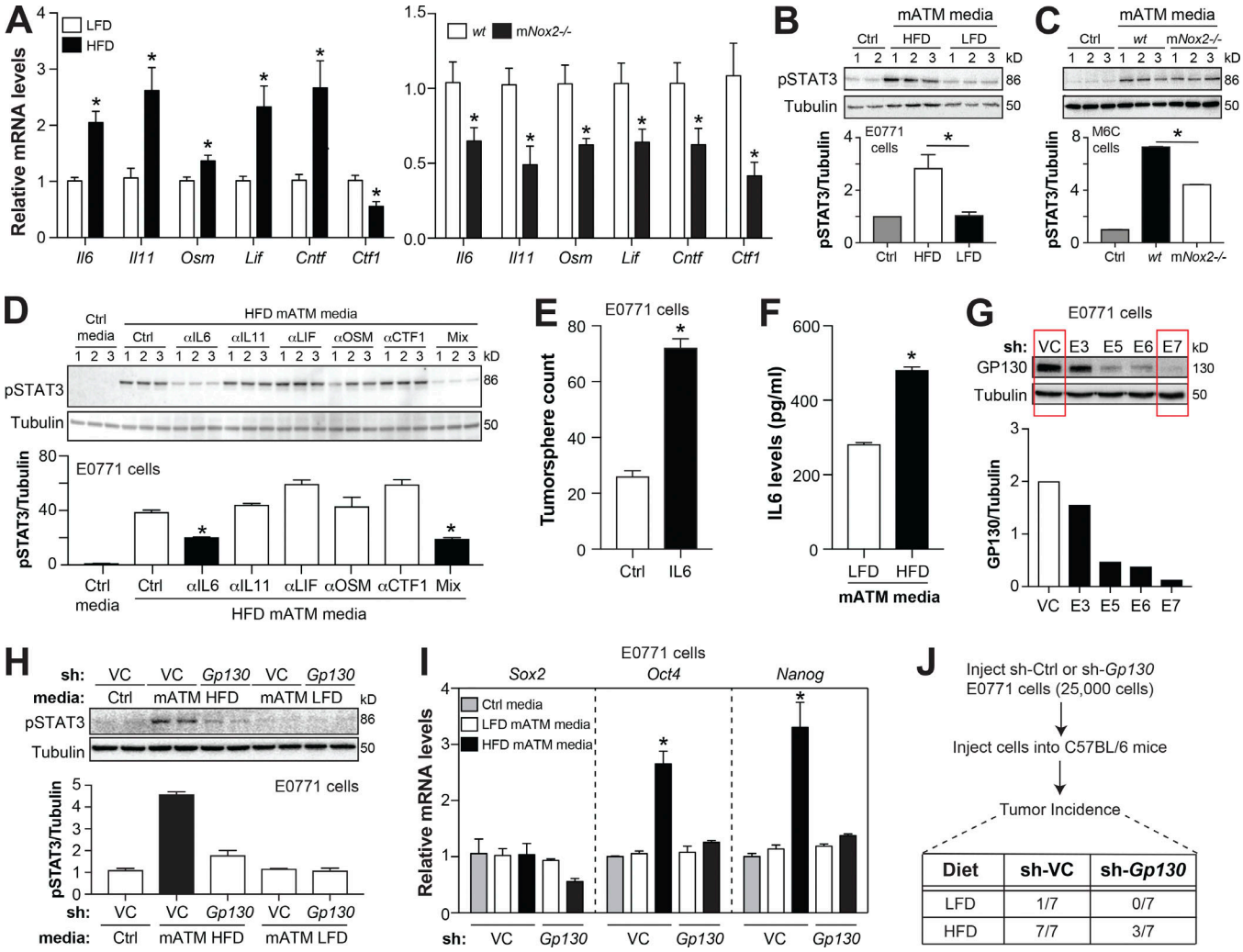

Figure 5. **MMe macrophage-derived IL-6 signals through GP130 to drive TNBC cell stemness. (A)** GP130 ligand expression in mATMs isolated from lean and obese C57BL/6 mice (left) or obese WT and obese m*Nox2*$^{-/-}$ mice (right), *n* = 4/group. **(B and C)** STAT3 phosphorylation in E0771 cells exposed to mATM media from lean and obese C57BL/6 mice, *n* = 2 or 3/group (B) or M6C cells exposed to mATM media from obese WT and obese m*Nox2*$^{-/-}$ mice, *n* = 2 or 3/group (C). **(D)** GP130 ligands in obese mATM media were inactivated with antibodies, alone or in combination (Mix), and effects on STAT3 phosphorylation in E0771 cells were quantified, *n* = 3/group. **(E)** Effect of purified IL-6 (50 ng/ml) on E0771 cell tumorsphere formation, *n* = 4/group. **(F)** IL-6 levels in lean and obese mATM media were quantified by ELISA, *n* = 3/group. **(G)** E0771 cells were treated with vector control shRNA (VC) or *Gp130* shRNA (E3, E5, E6, and E7), and GP130 knockdown was confirmed by Western blotting. **(H and I)** Effect of GP130 knockdown (E7) on the ability of obese mATM media to induce STAT3 phosphorylation, *n* = 2/group (H) and stem cell marker expression in E0771 cells, *n* = 4/group (I). **(J)** Tumor incidence following injection of sh-VC or sh-Gp130 (E7) E0771 cells into mammary fat of lean or obese C57BL/6 mice, *n* = 7/group. Ctrl, control. Results are mean ± SEM. *, P < 0.05; Student's *t* test.

mammary fat, even though body weight and mammary and visceral fat mass remained significantly elevated relative to lean mice.

Human MMe macrophages are present in mammary adipose tissue of obese women

Having shown that MMe macrophages are an important mechanism by which obesity promotes TNBC tumor initiation in mice, we investigated whether this mechanism may also be operative in humans. Three approaches were used to test this possibility.

First, we investigated whether MMe macrophages were increased in mammary adipose tissue of obese women (body mass index [BMI] >30 kg/m^2) in comparison to nonobese women (BMI <30 kg/m^2) undergoing mammary reductions. To this end, we isolated the SVCs from mammary adipose tissue and studied ATMs (defined as CD45$^+$CD11b$^+$CD14$^+$) by flow cytometry.

The number of ATMs (defined as CD45$^+$CD11b$^+$CD14$^+$) in the SVC from mammary fat was significantly elevated in obese women relative to nonobese women (Fig. 7 A and Fig. S1). To explore the activation status of mATMs, we stained them with antibodies against M1 markers (CD319 and CD38) and MMe macrophages (ABCA1 and CD36). These analyses showed that MMe ATMs, and not M1 ATMs, accumulate in mammary adipose tissue during obesity (Fig. 7 A). Indeed, the percentage of mATMs expressing MMe markers was significantly and positively correlated with BMI (P < 0.001, R^2 = 0.67), while the

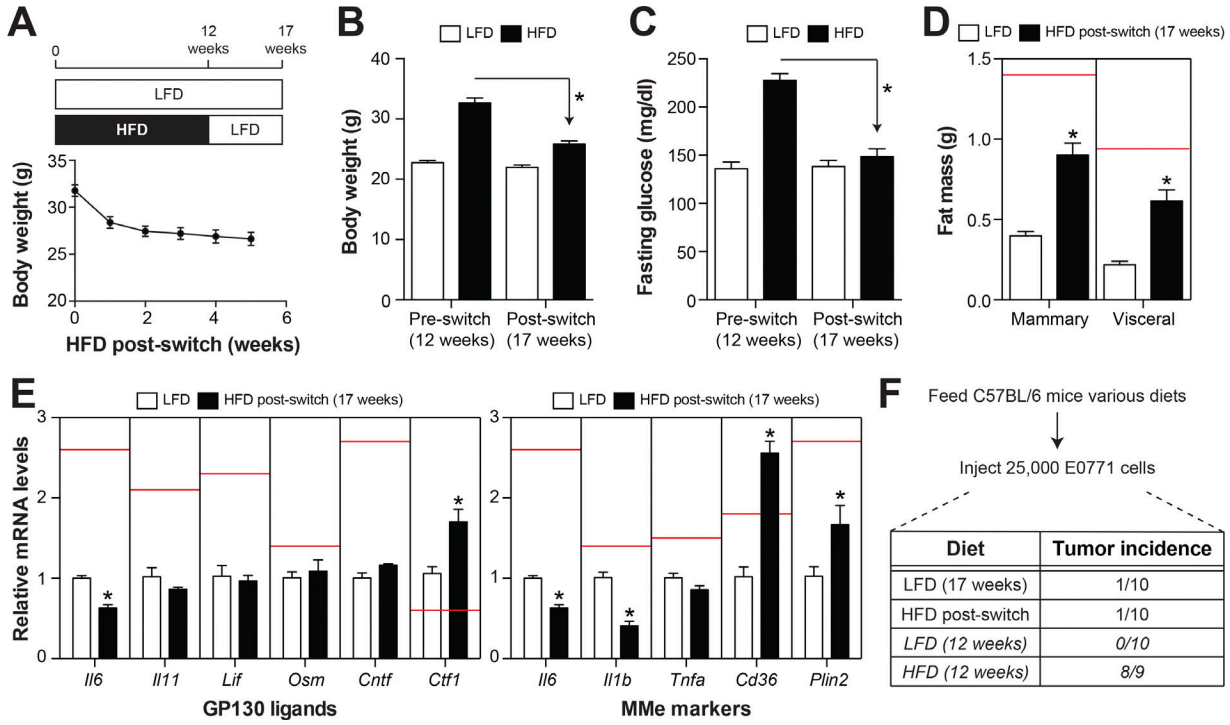

Diet	Tumor incidence
LFD (17 weeks)	1/10
HFD post-switch	1/10
LFD (12 weeks)	*0/10*
HFD (12 weeks)	*8/9*

Figure 6. **Weight loss reduces MMe macrophage inflammation and TNBC tumor formation. (A)** Female C57BL/6 mice were fed a LFD (control) or HFD for 12 wk. At this time, obese mice were switched to a LFD for 5 wk to induce stable weight loss (HFD switch), n = 10/group. **(B and C)** Body weight, n = 10/group (B) and fasting glucose levels, n = 10/group (C) were monitored before and after diet switch. **(D and E)** Mammary and visceral adipose tissue weight, n = 10/group (D), as well as GP130 ligand expression and MMe marker expression in purified mATMs, n = 4/group (E) were quantified after switch at 17 wk. Red lines indicate values obtained from C57BL/6 mice fed a HFD for 12 wk, which are represented from Fig. 4 to facilitate comparison. **(F)** Tumor incidence following injection of E0771 cells into mammary fat, n = 9–10/group. Tumor incidence at 12 wk of LFD and HFD is represented from Fig. 1 for comparative purposes. Results are mean ± SEM. *, $P < 0.05$; Student's t test.

percentage of M1 ATMs was not correlated ($P = 0.14$, $R^2 = 0.14$; Fig. 7 B).

Interestingly, the expression levels of MMe markers on mATMs were not different in lean and obese subjects (Fig. S1). Instead, we observed an increase in the number of MMe macrophages in the SVC of obese mammary fat. These data are in contrast to what we observed in mammary adipose tissue in mice, where obesity induced MMe marker expression in ATMs without altering their number (see Fig. 2). Although the mechanisms are different between mice and humans, the common endpoint is an increased presence of MMe macrophages in mammary adipose tissue during obesity.

Second, we determined whether human mATMs could signal through GP130 to promote human TNBC cell stem-like properties. Because we were unable to isolate enough ATMs from mammary adipose tissue of lean subjects, and the number of purified mATMs from obese subjects (Fig. 7 C) was limiting, we could only test this hypothesis using a limited number of assays. We found that mATM-conditioned media, collected from three obese women, induced STAT3 phosphorylation and stem cell marker expression in SUM159 cells (Fig. 7, E and F), a human TNBC cell line (Neve et al., 2006). Importantly, both of these effects were diminished when GP130 was knocked down in SUM159 cells by shRNA (Fig. 7, D–F).

To provide additional evidence that human MMe macrophages can support GP130-mediated stemness in TNBC cells, we isolated human monocyte-derived macrophages (M0) and exposed them to MMe-polarizing stimuli in vitro. In vitro–derived human MMe macrophages overexpressed all GP130 ligands tested, including *IL6*, *OSM*, *CNTF*, *CTF1*, and *LIF* (Fig. 7 G). Moreover, human MMe macrophage media induced STAT3 phosphorylation, stem cell marker expression, and tumorsphere growth of SUM159 cells, and all of these effects were attenuated by GP130 knockdown (Fig. 7, H–J).

Third, we determined whether obesity was associated with increased nuclear pSTAT3 in breast cancer patients with DCIS, a noninvasive stage that is representative of the tumor initiation step studied in our preclinical mouse models. Tissue microarrays (TMAs) were obtained from lean (BMI <25 kg/m^2, n = 8), overweight (BMI 25–30 kg/m^2, n = 9), and obese (BMI >30 kg/m^2, n = 9) patients. TMA sections were stained with an anti-pSTAT3 antibody, and nuclear localization and intensity were quantified according to the Allred score (Allred et al., 1998). Results were consistent with increased STAT3 phosphorylation in the tumors of both overweight and obese patients relative to lean patients (Fig. 7 K and Fig. S3).

Collectively, these findings suggest that during obesity, MMe macrophages accumulate in mammary adipose tissue, and that human MMe macrophages, like their mouse counterparts, can promote stem-like properties in TNBC cells through GP130 signaling.

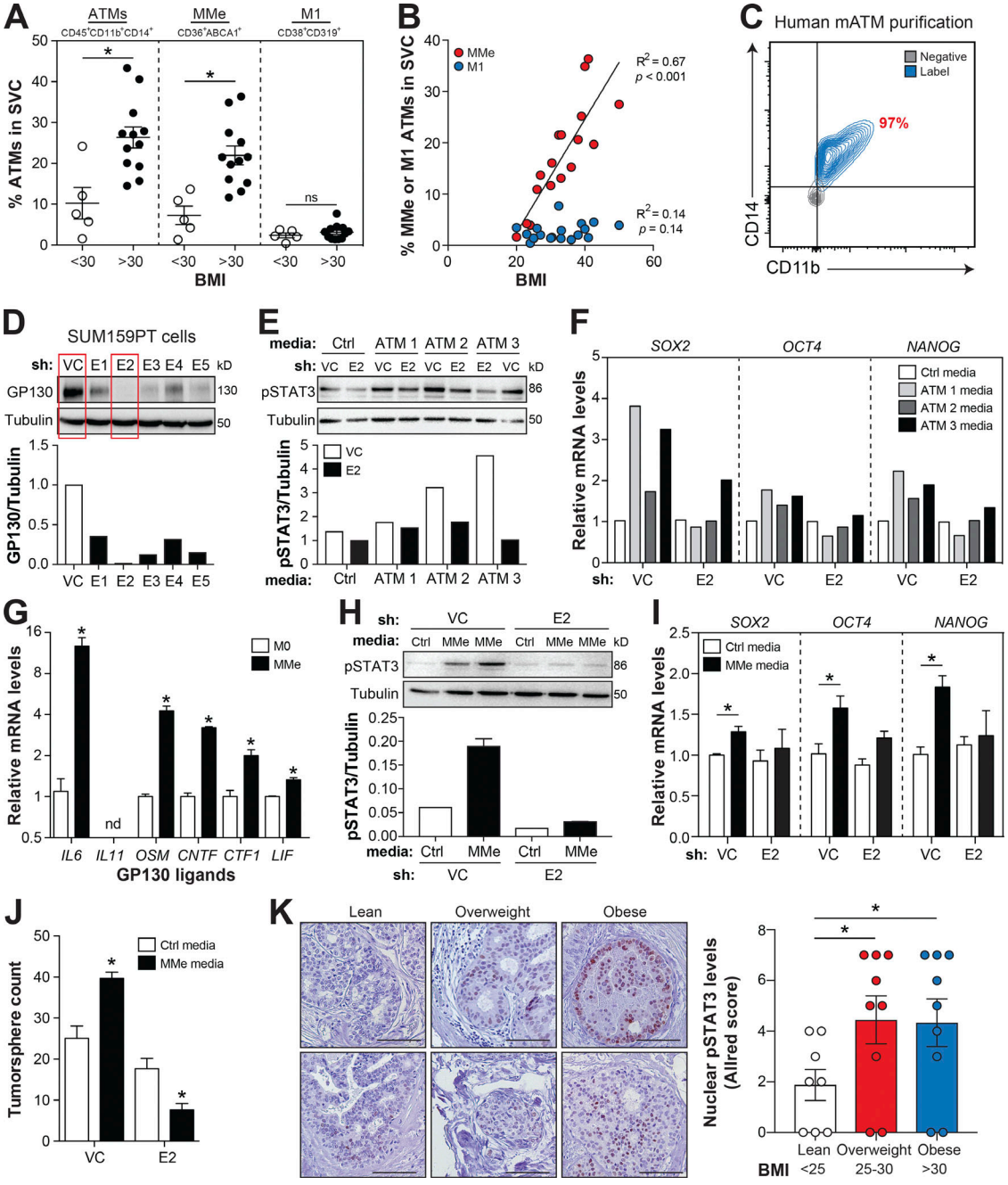

Figure 7. **MMe macrophages are present in mammary fat of obese women and promote stem-like properties in TNBC cells. (A)** SVCs were isolated from mammary fat, and the percentages of ATMs, MMe ATMs, and M1 ATMs were quantified by flow cytometry, *n* = 5–12/group. **(B)** Linear regression analysis of percentages of MMe and M1 ATMs in mammary fat with BMI. **(C)** Purification of mATMs from obese women. **(D)** Human SUM159PT cells were treated with control shRNA (VC) or *GP130* shRNA (E1–E5), and GP130 knockdown was confirmed by Western blotting. **(E and F)** Effect of *GP130* knockdown (E2) on the ability of obese mATM media, from three independent donors, to induce STAT3 phosphorylation (E) and stem cell marker expression (F) in SUM159PT cells. **(G)** GP130 ligand expression in unstimulated (M0) and MMe human monocyte–derived macrophages, *n* = 3/group. **(H–J)** Effect of *GP130* knockdown (E2) on the ability of human MMe media to induce STAT3 phosphorylation, *n* = 1–2/group (H), stem cell marker expression, *n* = 3/group (I), and tumorsphere formation, *n* = 3/group (J), in SUM159PT cells. **(K)** Mammary adipose tissue obtained from lean (BMI <25, *n* = 8), overweight (BMI 25–30, *n* = 9), and obese (BMI >30, *n* = 9) breast cancer patients with DCIS was stained with an anti-pSTAT3 antibody (brown) and counterstained with hematoxylin (blue), and the intensity and percentage of nuclear pSTAT3-positive cells were quantified according to the Allred score. Bar, 100 µm. Ctrl, control; nd, not detected. Results are mean ± SEM. *, P < 0.05; Student's *t* test.

Discussion

Our findings support a model wherein DIO induces an MMe phenotype in mATMs, which overexpress cytokines that signal through GP130 to induce stem-like properties in TNBC cells. Three lines of evidence support the idea that MMe mATMs promote TNBC tumor formation during obesity. First, we show that MMe is the predominant ATM phenotype in mammary adipose tissue of obese humans and mice. Second, we

demonstrate that in vitro–derived murine and human MMe macrophages mimic the effects of obese mATMs on stem-like properties of TNBC cells, both in terms of mechanism and function. Third, we show that ablating *Nox2*, a gene required for MMe macrophage polarization, attenuated the ability of obese mATMs to promote TNBC stemness in vitro, and the ability of obesity to promote TNBC tumor formation in vivo. The importance of this mechanism is underscored by our demonstration that it is used by in vitro– and in vivo–derived MMe macrophages to induce stem-like properties in multiple TNBC cell lines of murine and human origin.

These findings, together with our previous work (Kratz et al., 2014), suggest that the MMe phenotype may be broadly applicable to ATMs in multiple adipose tissue depots during obesity in humans and mice, and that these cells perform a wide array of functions that impact the metabolic phenotype and its associated comorbidities. We previously showed that MMe-like ATMs in visceral fat overexpress inflammatory cytokines to exacerbate insulin resistance during early obesity, but also protect against insulin resistance in prolonged obesity by clearing dead adipocytes through a lysosomal exocytosis pathway (Coats et al., 2017). Our new findings suggest that MMe-like ATMs in mammary fat overexpress GP130 ligands that promote TNBC stem-like properties, and it is possible that a similar MMe macrophage mechanism may promote estrogen receptor–positive (ER^+) breast cancer and other obesity-associated cancers arising in adipose tissue–rich environments (e.g., ovarian, colon, and brain). However, deciphering the contribution of MMe macrophages in ER^+ breast cancer may be challenging because obesity is also known to promote ER^+ breast cancer by increasing local production of estrogen in adipose tissue (Subbaramaiah et al., 2011).

Cancer cells with stem-like properties are known to promote tumor initiation and metastasis (Grivennikov et al., 2010). These stem-like properties may be activated by mutation of key genes or epigenetic regulators in cancer cells, or by signals from the tumor microenvironment (Karnoub et al., 2007; Liu et al., 2011). Inflammatory cytokines (such as IL-6) arising from tumor cells or an altered tumor microenvironment can signal through GP130 to induce JAK/STAT signaling and drive cancer cell stemness (Korkaya et al., 2011; Lu et al., 2014). Constitutively activated STAT3 has been implicated in the initiation of many types of cancer, including breast cancer (Ling and Arlinghaus, 2005), as well as the promotion of invasion, migration, epithelial-to-mesenchymal transition, and cancer stem cell self-renewal and differentiation (Korkaya et al., 2011; Yuan et al., 2015). Indeed, we show that pSTAT3 levels are elevated in overweight and obese breast cancer patients with early DCIS. However, we could not correlate this increase with MMe macrophage levels or location in adipose tissue because MMe markers (PLIN2, ABCA1, and CD36) are also highly expressed by adipocytes, highlighting the need for deeper proteomics studies to identify more selective MMe markers in the future. Our findings suggest that the chronic metabolic activation of ATMs in mammary fat promotes TNBC tumor formation through this mechanism and could contribute to metastatic progression as well.

Importantly, disabling this MMe-GP130–stemness pathway (by deleting *Nox2* in macrophages or attenuating *Gp130* in TNBC cells) did not completely block increased tumor formation during obesity. It is therefore likely that additional DIO-induced factors can contribute to this phenotype. For example, leptin, an adipocyte-derived hormone that is increased during obesity, has been shown to promote cancer cell stemness in breast cancer (Chang et al., 2015). FFAs can also promote stem-like properties in cancer cells (Ye et al., 2016), and the increased adipose tissue mass and adipocyte insulin resistance would increase FFA levels in mammary adipose tissue during obesity. These increased FFA levels would also stimulate MMe polarization in mATMs, which our findings suggest substantially contributes to TNBC cell stemness during obesity.

More generally, our findings reinforce the idea that tumorigenesis is regulated both by intrinsic properties of cancer cells (i.e., genetic alterations) and by the tissue-specific niche in which the tumor develops (Polyak et al., 2009). From this perspective, obesity may be conceptualized as a pathological state that facilitates tumorigenesis by creating tumor permissive conditions in multiple tissues. For example, our studies demonstrated that obesity-induced ATM inflammation in mammary fat promotes TNBC tumor formation, while previous studies showed that obesity-induced neutropenia in the airway facilitates TNBC tumor metastasis (Quail et al., 2017). Although the specific mechanisms underlying these observations are distinct, they can be integrated through obesity's ability to induce chronic inflammation. Notably, our studies combined with previous work (Quail et al., 2017) suggest that this chronic inflammation and its effects on tumorigenesis may be reversed by caloric restriction, highlighting the potential therapeutic value of weight loss intervention.

Chronic inflammation, from a multitude of underlying sources, is known to promote cancer cell stemness and increase the risk of many types of cancers (Multhoff et al., 2012). For example, epidemiological studies have linked ulcerative colitis, hepatitis C, and chronic pancreatitis to the development of cancers of the colon, liver, and pancreas. Similarly, obesity has been shown to induce inflammation in mammary adipose tissue (Howe et al., 2013; Vaysse et al., 2017), and our results show that MMe macrophages are a key source of this inflammation.

The mechanism by which MMe macrophages induce stem-like phenotypes in tumor cells reveals a number of potential therapeutic approaches to counteract the effects of obesity. NOX2 inhibitors such as gp91sd-tat (Smith et al., 2015) may be an attractive approach for attenuating MMe macrophage inflammation in obesity-driven TNBC. GP130 inhibitors such as bazedoxifene (Xu and Neamati, 2013) may also be useful for blocking the ability of MMe-derived cytokines to induce TNBC cell stemness. Finally, JAK1/2 inhibitors may have therapeutic value in blocking signaling downstream of MMe-derived cytokine interactions with GP130, and the JAK1/2 inhibitor ruxolitinib is currently in clinical trials for treatment of TNBC (Harrison et al., 2012). Future studies will be needed to test the efficacy of these therapeutics in treating obesity-associated TNBC.

Materials and methods

Regulatory approval

Animal studies were approved by the University of Chicago Institutional Animal Care and Use Committee (Animal Care and Use Procedure nos. 72209 and 72228). Human studies were approved by the Institutional Review Boards at the University of Chicago (IRB16-0321) and Northwestern University (NU 11B04).

Subject recruitment

Human breast adipose tissue was obtained from women undergoing breast reduction surgery surgeries at Northwestern Memorial Hospital. Exclusion criteria included cancer or any other breast-related diseases. Human breast adipose tissue was collected by surgeons, and tissue was processed immediately to obtain the SVCs for flow-cytometric analyses.

Mice

WT and *Nox2*$^{-/-}$ (*Cybb*$^{-/-}$) female mice on the C57BL/6 background, and C3(1)-TAg mice are from The Jackson Laboratory. m*Nox2*$^{-/-}$ mice were generated by crossing *Cybb*$^{fl/fl}$ mice with *LysM-cre* knock in mice (004781; The Jackson Laboratory) to generate LysM-cre$^{+/-}$ *Cybb*$^{fl/fl}$ and littermate control *Cybb*$^{fl/fl}$ mice as previously described (Coats et al., 2017). Mouse genotype was confirmed by PCR (see Table S1 for primers).

DIO studies

Female C57BL/6 or C3(1)-TAg female mice were placed on a LFD (Harlan) or 60% HFD (D12451; Research Diets Inc.) at 6 wk of age for 12 wk. Body weight was monitored every week.

Plasma metabolic measurements

Mice were fasted for 3 h, and blood glucose levels were measured with a One Touch Ultra 2 glucometer (Lifescan); serum insulin levels were measured by ELISA (Millipore).

TNBC cell lines

The TNBC cells lines used in this study include E0771 cells, originally isolated from a spontaneous breast adenocarcinoma in C57BL/6 mice (Casey et al., 1951); M6C cells, originally isolated from the C3(1)/SV40 Large T-antigen transgenic mouse model (Holzer et al., 2003); Py8119 cells, derived from a mammary adenocarcinoma that spontaneously arose in a MMTV-PyMT transgenic C57BL/6 female mouse (Gibby et al., 2012); and SUM159PT cells, derived from a primary TNBC tumor from a patient with invasive ductal carcinoma (Neve et al., 2006). Py8119 and SUM159PT cells were obtained from the American Type Culture Collection and cultured according to their guidelines. All other cells were maintained in DMEM supplemented with 10% FCS.

Cancer cell isolation from tumors

Tumors were digested with collagenase and hyaluronidase (1:3) and 0.1 mg/ml DNase I (Worthington), filtered through 70-µm mesh, incubated with RBC lysis buffer, filtered through 40-µm mesh, and resuspended in PBS with 1% BSA. To isolate cancer cells for quantitative RT-PCR (qRT-PCR) analysis, mononuclear cells were depleted by centrifuging using Ficoll-Paque PREMIUM, with a density of 1.077 ± 0.001 g/ml for 40 min at 400 ×*g* after RBC lysis. The pellet at the bottom was resuspended in RNeasy lysis buffer (Qiagen) for RNA isolation. For assessment of surface CD90 levels by cancer cells isolated from C3(1)-TAg tumors, CD45^{-}CD31^{-}Ter119^{-} cells (i.e., negative for immune and endothelial cell markers) were analyzed for CD90 levels by flow cytometry.

Murine adipose tissue staining

6-wk-old C3(1)-TAg mice were fed an LFD or HFD for 6 wk. Mammary adipose tissue was isolated at 12 wk of age, a time point that coincides with DCIS (Holzer et al., 2003). Adipose tissue was sectioned (5 µm), stained with anti-F4/80 antibody (Abcam) to visualize ATMs, and counterstained with hematoxylin. Images were acquired with a Nikon Eclipse Ti2 microscope with the following setting: brightfield, objective magnification 20 and objective numerical aperture 0.45, room temperature, Color Camera Nikon DS-Ri2, and NIS-Element Version 5.02 software.

Mammary and visceral fat was obtained from WT and m*Nox2*$^{-/-}$ mice fed a LFD or HFD for 10 wk. Adipose tissue was sectioned (5 µm) and stained with antibodies against MAC2 (Cedarlane) and PLIN2 (Abcam). Fluorescence images were acquired with a Nikon Eclipse Ti2 microscope with the following setting: objective magnification 20, objective numerical aperture 0.45, room temperature, emission wavelength of DAPI (457.5 nm), GFP (535.0 nm), and RFP (610 nm), Camera Nikon DS-Qi2, and NIS-Element Version 5.02 software.

Immunohistochemistry of pSTAT3 in human breast tumors

Archival formalin-fixed and paraffin-embedded tissues of breast cancer patients with DCIS were obtained from the surgical pathology archive at the University of Chicago. TMAs were constructed from formalin-fixed, paraffin-embedded tumor samples (DCIS and adjacent normal). MCF-7 cells were pelleted and processed by formalin-fixation and paraffin-embedding and served as positive control. Cores were precisely arrayed into a new recipient paraffin block using an automated arrayer (ATA-27; Beecher Instruments). Documentation of location for each tissue core was performed on ready-made grids using Microsoft Excel.

TMA tissue sections (4 µm) were deparaffinized in xylene and rehydrated through a graded alcohol series to distilled water, cooled to room temperature, and washed in Tris-buffered saline. Antigen retrieval was performed in a vegetable steamer in Universal Decloaker target retrieval solution (BioCare Medical). Slides were incubated in Peroxidazed 1 (BioCare Medical) for 10 min to block endogenous peroxidase activity, followed by incubation for 15 min in Background Sniper (BioCare Medical) to reduce nonspecific background. TMA sections were stained with an anti-pY705-STAT3 antibody (dilution 1:25; ab76315; Abcam) and detected with the BioCare Medical Polymer Detection Kit (M3R531G). Slides were then treated for 5 min with 3–3′-diaminobenzidine chromogen and counterstained with hematoxylin. Images were acquired with a Leica DMLB microscope with the following settings: brightfield, objective magnification 20, numerical aperture of the objective lens 0.45, room

temperature, Leica FFC450 camera, and Leica Application Suite V3.8 software.

Immunostaining was scored semi-quantitatively according to the Allred score as previously described (Allred et al., 1998). Briefly, scoring was based on intensity of pSTAT3 signal (on a scale of 0 to 3) and percentage of positively stained nuclei (on a scale of 0 to 5) for a total score of 0 to 8. Final score 0–2 was considered as negative, and final score 3–8 was considered as positive.

ATM isolation and analysis

SVC was obtained by digesting human or mouse mammary adipose tissue with collagenase type 2 for 60 min and filtering the supernatant with a 40-µm filter after RBC lysis. mATMs in the SVC obtained from murine and human mammary fat were interrogated by flow cytometry (see Fig. S1 for the gating strategy). Murine and human mATMs were isolated using anti-CD11b antibody coupled to magnetic beads as previously described (Kratz et al., 2014), and purity was assessed by flow cytometry. ATMs were interrogated by qRT-PCR, and media was collected for functional assays.

Differentiation and metabolic activation of murine bone marrow–derived macrophages (BMDMs) and human monocyte-derived macrophages

Murine BMDMs were generated and metabolically activated as previously described (Kratz et al., 2014). Briefly, bone marrow was flushed from the bones of the hind legs and differentiated to macrophages by culturing for 6 d in six-well plates in DMEM with 10% FCS plus conditioned media from L929 cells at a 1:3 ratio. Human peripheral blood monocytes were isolated from healthy donors and differentiated to macrophages in the presence of M-CSF (125 ng/ml). For MMe activation, macrophages were treated with glucose (30 mM), insulin (10 nM), and palmitate (0.3 mM) for 24 h. Conditioned media were generated by culturing primary immune cells in regular DMEM serum-free media for 24 h, using 0.6 ml of media for every 1 million macrophages seeded.

Limiting dilution assays

E0771 or PY8119 cells were transplanted into the no. 4 mammary fat pad. Tumors were considered established when they became palpable for two consecutive weeks. Analyses of tumor incidence were confirmed by two independent investigators. To test the effects of ATMs or MMe macrophages on E0771 tumor-initiating potential, we serum-starved the cells overnight, treated them with macrophage-conditioned media for 24 h in DMEM supplemented with 2.5% FBS, counted the cells, and injected them into the mammary fat pad.

Tumorsphere assays

E0771, M6C, or SUM159PT cells were plated at 500 cells/well of a ultra-low attachment 12-well plate (Corning) in standard mammosphere media comprising DMEM-F12 supplemented with fibroblast growth factor (20 ng/ml; GoldBio), epidermal growth factor (20 ng/ml; GoldBio), heparin (4 mg/ml; Sigma-Aldrich) and B27 supplement (Life Technologies). Tumorspheres were counted following 5–8 d of growth. To study the effects of macrophage media on tumorsphere formation, tumor cells were pretreated with macrophage-conditioned media for 48 h in DMEM supplemented with 2.5% serum. At this time, cells were collected, counted, and plated for tumorsphere assays. To study the effects of macrophage media on tumorsphere formation, tumor cells were serum-starved overnight and pretreated with macrophage-conditioned media for 24 h in DMEM supplemented with 2.5% serum. For cytokine neutralization studies, obese mATM media were treated with anti–IL-6 (100 ng/ml; R&D Systems), anti–IL-11 (100 ng/ml; R&D Systems), anti-LIF (100 ng/ml; R&D Systems) or anti-OSM (100 ng/ml; R&D Systems) antibodies, alone or in combination, for 20 min before adding the media to TNBC cells. For serial propagation studies, tumorspheres were trypsinized to obtain single cells, and resuspended in mammosphere media. Cells were counted and replated at 200 cells/well, and tumorsphere formation was assessed in the absence of any treatments.

GP130 knockdown

shRNA specific for murine or human *Gp130* ligated into the lentiviral vector pLKO-1 was purchased from Dhramacon. Virus particles were packaged, E0771 and SUM159PT cells were infected, and infected cells were selected for by treatment with puromycin. Lentiviral pLKO-1 vector without shRNA was used as a control. Knockdown of GP130 was verified by immunoblotting.

Antibodies

Antibodies for flow-cytometric measurements of murine cells were CD90, CD45, CD11b, CD206, CD14, CD36, CD38, CD319, F4/80, CD3, CD4, and CD8 (BD Biosciences), ABCA1 (Novus Biologicals), and CD24 (Biolegend). Antibodies for flow-cytometric measurements of human cells were CD45, CD11b, CD206, CD14, CD36, CD38, CD319 (BD Biosciences), and ABCA1 (Novus Biologicals).

Western blotting

Cancer cells were lysed with 1% SDS containing protease and phosphatase inhibitors (Sigma-Aldrich), and protein was quantified with the BCA Protein Assay Kit (Pierce). Proteins (10–20 µg) were resolved on 7.5% SDS-PAGE gels, transferred to polyvinylidene fluoride membranes (Millipore), blocked with 5% milk at room temperature for 2 h, stained with anti-human and murine pSTAT3 (Y705; Cell Signaling) or anti-human and murine tubulin (Santa Cruz Biotechnology) antibodies, and quantified using the enhanced chemiluminescence detection kit (Bio-Rad) and a LI-COR imager.

Statistics

Unless otherwise stated, statistical significance was assessed using an unpaired, two-tailed Student's *t* test. Statistical significance for tumor initiation studies was assessed with the ELDA software (Hu and Smyth, 2009). Replicate numbers for each experiment are indicated in the figure legends.

qRT-PCR

RNA was isolated using Qiagen Midi-prep kits and reverse-transcribed with Quantiscript (Qiagen) using random hexamers

(Invitrogen), and mRNA levels were measured with specific primers (Table S1) using SYBR green on a One Step Plus system (Applied Biosystems). Relative levels of each target gene were calculated using the ΔΔCt formula, using 18S RNA as a control.

Online supplemental material

Fig. S1 demonstrates our flow cytometry analytical approach and raw data for quantifying mammary fat ATMs and cancer cell stemness. Fig. S2 shows that DIO decreases the latency of E0771 and Py8119 tumors. Fig. S3 provides representative microscopy images to support findings reported in the main figures. Fig. S4 demonstrates that in vitro–derived murine MMe macrophages release factors that signal through GP130 to promote stem-like properties in TNBC cells. Table S1 provides a list of all primer sequences used for qRT-PCR and genotyping.

Acknowledgments

We would like to thank Drs. Ramesh Ganju (Ohio State University, Columbus, OH) and Jeffrey Green (National Cancer Institute, Bethesda, MD) for providing the E0771 and M6C cell lines, respectively.

This research was supported by grants from the National Institutes of Health (R01DK102960, R01CA184494, R01DK107868, P30DK020595, and F99CA212477), the Cancer Research Foundation, the Avon Foundation, the Bernice Goldblatt Endowment Fellowship, the University of Chicago, and the Department of Health via a National Institute for Health Research Biomedical Research Centre award to Guy's and St Thomas' NHS Foundation Trust and Kings College London.

The authors declare no competing financial interests.

Author contributions: Conceptualization: L. Becker, M.R. Rosner, and P. Tiwari. Investigation: P. Tiwari, A. Blank, C. Cui, G. Zhou, K.Q. Schoenfelt, Y. Xu, and G. Khramtsova. Writing, original draft: L. Becker, M.R. Rosner, and P. Tiwari. Writing, reviewing and editing: All authors. Supervision: L. Becker, M.R. Rosner, S.A. Khan, and F. Olopade. Funding acquisition: L. Becker, M.R. Rosner, and S.A. Khan.

Submitted: 22 August 2018
Revised: 27 January 2019
Accepted: 29 March 2019

References

Allred, D.C., J.M. Harvey, M. Berardo, and G.M. Clark. 1998. Prognostic and predictive factors in breast cancer by immunohistochemical analysis. *Mod. Pathol.* 11:155–168.

Calle, E.E., C. Rodriguez, K. Walker-Thurmond, and M.J. Thun. 2003. Overweight, obesity, and mortality from cancer in a prospectively studied cohort of U.S. adults. *N. Engl. J. Med.* 348:1625–1638. https://doi.org/10.1056/NEJMoa021423

Casey, A.E., W.R. Laster Jr., and G.L. Ross. 1951. Sustained enhanced growth of carcinoma EO771 in C57 black mice. *Proc. Soc. Exp. Biol. Med.* 77:358–362. https://doi.org/10.3181/00379727-77-18779

Celià-Terrassa, T., D.D. Liu, A. Choudhury, X. Hang, Y. Wei, J. Zamalloa, R. Alfaro-Aco, R. Chakrabarti, Y.Z. Jiang, B.I. Koh, et al. 2017. Normal and cancerous mammary stem cells evade interferon-induced constraint through the miR-199a-LCOR axis. *Nat. Cell Biol.* 19:711–723. https://doi.org/10.1038/ncb3533

Chakrabarti, R., T. Celià-Terrassa, S. Kumar, X. Hang, Y. Wei, A. Choudhury, J. Hwang, J. Peng, B. Nixon, J.J. Grady, et al. 2018. Notch ligand Dll1 mediates cross-talk between mammary stem cells and the macrophageal niche. *Science.* 360:eaan4153. https://doi.org/10.1126/science.aan4153

Chan, D.S., and T. Norat. 2015. Obesity and breast cancer: not only a risk factor of the disease. *Curr. Treat. Options Oncol.* 16:22. https://doi.org/10.1007/s11864-015-0341-9

Chang, C.C., M.J. Wu, J.Y. Yang, I.G. Camarillo, and C.J. Chang. 2015. Leptin-STAT3-G9a Signaling Promotes Obesity-Mediated Breast Cancer Progression. *Cancer Res.* 75:2375–2386. https://doi.org/10.1158/0008-5472.CAN-14-3076

Choi, Y., S.K. Park, K.J. Ahn, H. Cho, T.H. Kim, H.K. Yoon, and Y.H. Lee. 2016. Being Overweight or Obese Increases the Risk of Progression in Triple-Negative Breast Cancer after Surgical Resection. *J. Korean Med. Sci.* 31:886–891. https://doi.org/10.3346/jkms.2016.31.6.886

Coats, B.R., K.Q. Schoenfelt, V.C. Barbosa-Lorenzi, E. Peris, C. Cui, A. Hoffman, G. Zhou, S. Fernandez, L. Zhai, B.A. Hall, et al. 2017. Metabolically Activated Adipose Tissue Macrophages Perform Detrimental and Beneficial Functions during Diet-Induced Obesity. *Cell Reports.* 20:3149–3161. https://doi.org/10.1016/j.celrep.2017.08.096

Dorfman, M.D., J.E. Krull, J.D. Douglass, R. Fasnacht, F. Lara-Lince, T.H. Meek, X. Shi, V. Damian, H.T. Nguyen, M.E. Matsen, et al. 2017. Sex differences in microglial CX3CR1 signalling determine obesity susceptibility in mice. *Nat. Commun.* 8:14556. https://doi.org/10.1038/ncomms14556

Gibby, K., W.K. You, K. Kadoya, H. Helgadottir, L.J. Young, L.G. Ellies, Y. Chang, R.D. Cardiff, and W.B. Stallcup. 2012. Early vascular deficits are correlated with delayed mammary tumorigenesis in the MMTV-PyMT transgenic mouse following genetic ablation of the NG2 proteoglycan. *Breast Cancer Res.* 14:R67. https://doi.org/10.1186/bcr3174

Green, J.E., M.A. Shibata, K. Yoshidome, M.L. Liu, C. Jorcyk, M.R. Anver, J. Wigginton, R. Wiltrout, E. Shibata, S. Kaczmarczyk, et al. 2000. The C3(1)/SV40 T-antigen transgenic mouse model of mammary cancer: ductal epithelial cell targeting with multistage progression to carcinoma. *Oncogene.* 19:1020–1027. https://doi.org/10.1038/sj.onc.1203280

Grivennikov, S.I., F.R. Greten, and M. Karin. 2010. Immunity, inflammation, and cancer. *Cell.* 140:883–899. https://doi.org/10.1016/j.cell.2010.01.025

Gyorki, D.E., M.L. Asselin-Labat, N. van Rooijen, G.J. Lindeman, and J.E. Visvader. 2009. Resident macrophages influence stem cell activity in the mammary gland. *Breast Cancer Res.* 11:R62. https://doi.org/10.1186/bcr2353

Harrison, C., J.J. Kiladjian, H.K. Al-Ali, H. Gisslinger, R. Waltzman, V. Stalbovskaya, M. McQuitty, D.S. Hunter, R. Levy, L. Knoops, et al. 2012. JAK inhibition with ruxolitinib versus best available therapy for myelofibrosis. *N. Engl. J. Med.* 366:787–798. https://doi.org/10.1056/NEJMoa1110556

Holzer, R.G., C. MacDougall, G. Cortright, K. Atwood, J.E. Green, and C.L. Jorcyk. 2003. Development and characterization of a progressive series of mammary adenocarcinoma cell lines derived from the C3(1)/SV40 Large T-antigen transgenic mouse model. *Breast Cancer Res. Treat.* 77:65–76. https://doi.org/10.1023/A:1021175931177

Howe, L.R., K. Subbaramaiah, C.A. Hudis, and A.J. Dannenberg. 2013. Molecular pathways: adipose inflammation as a mediator of obesity-associated cancer. *Clin. Cancer Res.* 19:6074–6083. https://doi.org/10.1158/1078-0432.CCR-12-2603

Hu, Y., and G.K. Smyth. 2009. ELDA: extreme limiting dilution analysis for comparing depleted and enriched populations in stem cell and other assays. *J. Immunol. Methods.* 347:70–78. https://doi.org/10.1016/j.jim.2009.06.008

Karnoub, A.E., A.B. Dash, A.P. Vo, A. Sullivan, M.W. Brooks, G.W. Bell, A.L. Richardson, K. Polyak, R. Tubo, and R.A. Weinberg. 2007. Mesenchymal stem cells within tumour stroma promote breast cancer metastasis. *Nature.* 449:557–563. https://doi.org/10.1038/nature06188

Klonisch, T., E. Wiechec, S. Hombach-Klonisch, S.R. Ande, S. Wesselborg, K. Schulze-Osthoff, and M. Los. 2008. Cancer stem cell markers in common cancers - therapeutic implications. *Trends Mol. Med.* 14:450–460. https://doi.org/10.1016/j.molmed.2008.08.003

Korkaya, H., S. Liu, and M.S. Wicha. 2011. Regulation of cancer stem cells by cytokine networks: attacking cancer's inflammatory roots. *Clin. Cancer Res.* 17:6125–6129. https://doi.org/10.1158/1078-0432.CCR-10-2743

Kratz, M., B.R. Coats, K.B. Hisert, D. Hagman, V. Mutskov, E. Peris, K.Q. Schoenfelt, J.N. Kuzma, I. Larson, P.S. Billing, et al. 2014. Metabolic dysfunction drives a mechanistically distinct proinflammatory phenotype in adipose tissue macrophages. *Cell Metab.* 20:614–625. https://doi.org/10.1016/j.cmet.2014.08.010

Lee, C.H., C.C. Yu, B.Y. Wang, and W.W. Chang. 2016. Tumorsphere as an effective in vitro platform for screening anti-cancer stem cell drugs. *Oncotarget.* 7:1215–1226.

Ling, X., and R.B. Arlinghaus. 2005. Knockdown of STAT3 expression by RNA interference inhibits the induction of breast tumors in immunocompetent mice. *Cancer Res.* 65:2532–2536. https://doi.org/10.1158/0008-5472.CAN-04-2425

Liu, S., C. Ginestier, S.J. Ou, S.G. Clouthier, S.H. Patel, F. Monville, H. Korkaya, A. Heath, J. Dutcher, C.G. Kleer, et al. 2011. Breast cancer stem cells are regulated by mesenchymal stem cells through cytokine networks. *Cancer Res.* 71:614–624. https://doi.org/10.1158/0008-5472.CAN-10-0538

Lu, H., K.R. Clauser, W.L. Tam, J. Fröse, X. Ye, E.N. Eaton, F. Reinhardt, V.S. Donnenberg, R. Bhargava, S.A. Carr, and R.A. Weinberg. 2014. A breast cancer stem cell niche supported by juxtacrine signalling from monocytes and macrophages. *Nat. Cell Biol.* 16:1105–1117. https://doi.org/10.1038/ncb3041

Lumeng, C.N., and A.R. Saltiel. 2011. Inflammatory links between obesity and metabolic disease. *J. Clin. Invest.* 121:2111–2117. https://doi.org/10.1172/JCI57132

Lumeng, C.N., S.M. Deyoung, J.L. Bodzin, and A.R. Saltiel. 2007. Increased inflammatory properties of adipose tissue macrophages recruited during diet-induced obesity. *Diabetes.* 56:16–23. https://doi.org/10.2337/db06-1076

Montgomery, M.K., N.L. Hallahan, S.H. Brown, M. Liu, T.W. Mitchell, G.J. Cooney, and N. Turner. 2013. Mouse strain-dependent variation in obesity and glucose homeostasis in response to high-fat feeding. *Diabetologia.* 56:1129–1139. https://doi.org/10.1007/s00125-013-2846-8

Multhoff, G., M. Molls, and J. Radons. 2012. Chronic inflammation in cancer development. *Front. Immunol.* 2:98. https://doi.org/10.3389/fimmu.2011.00098

Mustafi, D., S. Fernandez, E. Markiewicz, X. Fan, M. Zamora, J. Mueller, M.J. Brady, S.D. Conzen, and G.S. Karczmar. 2017. MRI reveals increased tumorigenesis following high fat feeding in a mouse model of triple-negative breast cancer. *NMR Biomed.* 30:30. https://doi.org/10.1002/nbm.3758

Neve, R.M., K. Chin, J. Fridlyand, J. Yeh, F.L. Baehner, T. Fevr, L. Clark, N. Bayani, J.P. Coppe, F. Tong, et al. 2006. A collection of breast cancer cell lines for the study of functionally distinct cancer subtypes. *Cancer Cell.* 10:515–527. https://doi.org/10.1016/j.ccr.2006.10.008

Nguyen, L.V., R. Vanner, P. Dirks, and C.J. Eaves. 2012. Cancer stem cells: an evolving concept. *Nat. Rev. Cancer.* 12:133–143. https://doi.org/10.1038/nrc3184

Noy, R., and J.W. Pollard. 2014. Tumor-associated macrophages: from mechanisms to therapy. *Immunity.* 41:49–61. https://doi.org/10.1016/j.immuni.2014.06.010

Pierobon, M., and C.L. Frankenfeld. 2013. Obesity as a risk factor for triple-negative breast cancers: a systematic review and meta-analysis. *Breast Cancer Res. Treat.* 137:307–314. https://doi.org/10.1007/s10549-012-2339-3

Polyak, K., I. Haviv, and I.G. Campbell. 2009. Co-evolution of tumor cells and their microenvironment. *Trends Genet.* 25:30–38. https://doi.org/10.1016/j.tig.2008.10.012

Pyonteck, S.M., L. Akkari, A.J. Schuhmacher, R.L. Bowman, L. Sevenich, D.F. Quail, O.C. Olson, M.L. Quick, J.T. Huse, V. Teijeiro, et al. 2013. CSF-1R inhibition alters macrophage polarization and blocks glioma progression. *Nat. Med.* 19:1264–1272. https://doi.org/10.1038/nm.3337

Quail, D.F., O.C. Olson, P. Bhardwaj, L.A. Walsh, L. Akkari, M.L. Quick, I.C. Chen, N. Wendel, N. Ben-Chetrit, J. Walker, et al. 2017. Obesity alters the lung myeloid cell landscape to enhance breast cancer metastasis through IL5 and GM-CSF. *Nat. Cell Biol.* 19:974–987. https://doi.org/10.1038/ncb3578

Silver, J.S., and C.A. Hunter. 2010. gp130 at the nexus of inflammation, autoimmunity, and cancer. *J. Leukoc. Biol.* 88:1145–1156. https://doi.org/10.1189/jlb.0410217

Smith, R.M., P. Kruzliak, Z. Adamcikova, and A. Zulli. 2015. Role of Nox inhibitors plumbagin, ML090 and gp91ds-tat peptide on homocysteine thiolactone induced blood vessel dysfunction. *Clin. Exp. Pharmacol. Physiol.* 42:860–864. https://doi.org/10.1111/1440-1681.12427

Subbaramaiah, K., L.R. Howe, P. Bhardwaj, B. Du, C. Gravaghi, R.K. Yantiss, X.K. Zhou, V.A. Blaho, T. Hla, P. Yang, et al. 2011. Obesity is associated with inflammation and elevated aromatase expression in the mouse mammary gland. *Cancer Prev. Res. (Phila.).* 4:329–346. https://doi.org/10.1158/1940-6207.CAPR-10-0381

Trivers, K.F., M.J. Lund, P.L. Porter, J.M. Liff, E.W. Flagg, R.J. Coates, and J.W. Eley. 2009. The epidemiology of triple-negative breast cancer, including race. *Cancer Causes Control.* 20:1071–1082. https://doi.org/10.1007/s10552-009-9331-1

Vaysse, C., J. Lømo, Ø. Garred, F. Fjeldheim, T. Lofteroed, E. Schlichting, A. McTiernan, H. Frydenberg, A. Husøy, S. Lundgren, et al. 2017. Inflammation of mammary adipose tissue occurs in overweight and obese patients exhibiting early-stage breast cancer. *NPJ Breast Cancer.* 3:19. https://doi.org/10.1038/s41523-017-0015-9

Vona-Davis, L., D.P. Rose, H. Hazard, M. Howard-McNatt, F. Adkins, J. Partin, and G. Hobbs. 2008. Triple-negative breast cancer and obesity in a rural Appalachian population. *Cancer Epidemiol. Biomarkers Prev.* 17:3319–3324. https://doi.org/10.1158/1055-9965.EPI-08-0544

Wang, Q.A., C. Tao, R.K. Gupta, and P.E. Scherer. 2013. Tracking adipogenesis during white adipose tissue development, expansion and regeneration. *Nat. Med.* 19:1338–1344. https://doi.org/10.1038/nm.3324

Xu, S., and N. Neamati. 2013. gp130: a promising drug target for cancer therapy. *Expert Opin. Ther. Targets.* 17:1303–1328. https://doi.org/10.1517/14728222.2013.830105

Xu, H., G.T. Barnes, Q. Yang, G. Tan, D. Yang, C.J. Chou, J. Sole, A. Nichols, J.S. Ross, L.A. Tartaglia, and H. Chen. 2003. Chronic inflammation in fat plays a crucial role in the development of obesity-related insulin resistance. *J. Clin. Invest.* 112:1821–1830. https://doi.org/10.1172/JCI200319451

Xu, X., A. Grijalva, A. Skowronski, M. van Eijk, M.J. Serlie, and A.W. Ferrante Jr. 2013. Obesity activates a program of lysosomal-dependent lipid metabolism in adipose tissue macrophages independently of classic activation. *Cell Metab.* 18:816–830. https://doi.org/10.1016/j.cmet.2013.11.001

Ye, H., B. Adane, N. Khan, T. Sullivan, M. Minhajuddin, M. Gasparetto, B. Stevens, S. Pei, M. Balys, J.M. Ashton, et al. 2016. Leukemic Stem Cells Evade Chemotherapy by Metabolic Adaptation to an Adipose Tissue Niche. *Cell Stem Cell.* 19:23–37. https://doi.org/10.1016/j.stem.2016.06.001

Yuan, J., F. Zhang, and R. Niu. 2015. Multiple regulation pathways and pivotal biological functions of STAT3 in cancer. *Sci. Rep.* 5:17663. https://doi.org/10.1038/srep17663